A Low-Voltage and Fast-Response Infrared Spatial Light Modulator

*Fenglin Peng, Daming Xu, Haiwei Chen, and Shin-Tson Wu**

***College of Optics and Photonics, University of Central Florida, Orlando, FL 32816, USA**

Abstract

We report a low-voltage and fast-response polymer network liquid crystal (PNLC) infrared phase modulator. By optimizing the UV curing temperature and LC host, we achieved $V_{2\pi}$= 22.8V at λ=1.55μm and response time about 1ms. Such a PNLC-based spatial light modulator is useful for adaptive optics, adaptive lens, and laser beam steering.

Author Keywords

Liquid crystal, low operation voltage, spatial light modulator

1. Introduction

Liquid crystal (LC) spatial light modulators (SLMs) [1] have been widely used in adaptive optics [2], adaptive lens, laser beam control [3], and fiber-optic communication [4]. Low operation voltage for 2π phase change ($V_{2\pi}$) and fast response time are critical requirements for these applications. Most SLMs using a nematic LC has advantage in low $V_{2\pi}$, however, its response time is relatively slow (50-100 ms) [5]. Polymer network liquid crystal (PNLC) [6, 7] is a promising candidate for SLM because of its simple fabrication method, sub-millisecond response time, and large phase change. The main technical challenge of PNLC is high operation voltage $V_{2\pi}$ ~100V [8]. On the other hand, the commonly used high resolution liquid-crystal-on-silicon (LCoS) has a maximum voltage of 24V [9]. Therefore, to implement PNLC into LCoS for infrared SLM applications, we need to lower the $V_{2\pi}$ to 24V, while keeping fast response time.

In this paper, we demonstrate a reflective-mode PNLC phase modulator with $V_{2\pi}$ =22.6V at λ=1.55μm, which enables PNLC to be integrated into a high resolution LCoS SLM. Moreover, the response time is τ≈1.13ms at the room temperature (23°C), which is ~100X faster than the corresponding nematic SLM. To achieve such a low operation voltage while keeping fast response time, we investigated the curing temperature effects on domain size, which plays a critical role affecting the operation voltage and response time. A physical model was proposed to describe this correlation. Besides, we define a figure of merit (*FoM*) for comparing the LC hosts. For a given LC host, there is an optimal operation temperature for each PNLC, where *FoM* has a maximum value.

2. Experiment and Results.

To fabricate PNLCs, we prepared a precursor by mixing 92.5wt% of LC host (JC-BP07N, JNC), with 7.0 wt% of monomer (RM257, Merck) and 0.5 wt% of photo-initiator (BAPO, Genocure). We filled the precursor into homogeneous LC cells. The cell gap was controlled at ~11.8μm. The clearing point (T_c) of JC-BP07N is 87°C. If the curing temperature is close or higher than T_c, then the LC molecules will not align well with the rubbing directions, resulting in severe light scattering after polymerization. Thus, during UV curing process we controlled the curing temperature for each cell from 0°C to 70°C, respectively. Here, a UV light-emitting diode (LED) lamp (λ=385nm, Intensity is 300 mW/cm^2) was employed and the exposure time was one hour.

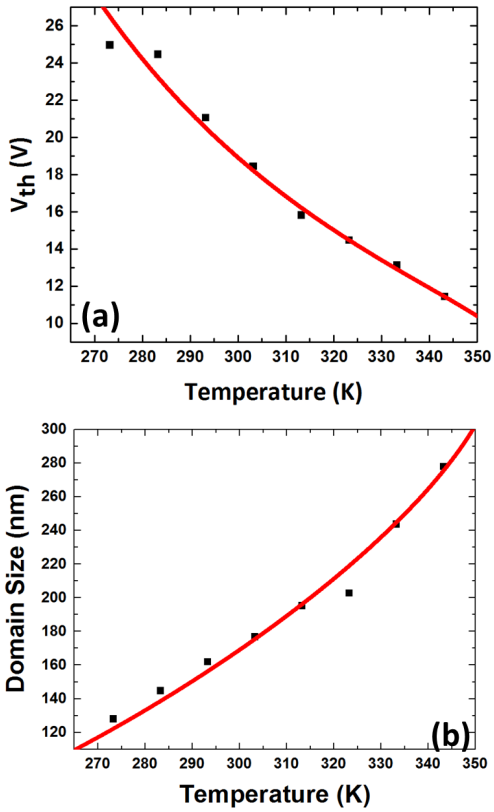

Figure 1 (a) Curing temperature dependent threshold voltage of PNLCs: dots stand for measured data and red line for fitting curve with Eq. (2). (b) Curing temperature dependent average domain size of PNLCs: dots stand for the measured data and red line for fitting curve with Eq. (3).

Curing Temperature Effects

To characterize the electro-optic properties of each PNLC cell, we measured its voltage-dependent transmittance (VT) with a laser beam at λ=1.55μm. The PNLC cells were sandwiched between two crossed polarizers, with the rubbing direction at 45° to the polarizer's transmission axis. The phase change of reflective mode is twice of transmissive mode due to the doubled optical path. Fig. 1(a) depicts the measured threshold voltage (V_{th}) of PNLCs cured at different temperatures. As the curing temperature increases from 0°C to 70°C, V_{th} decreases from 25.0V to 10.9V. This is because the LC viscosity decreases exponentially with increased curing temperature, which accelerates the polymer diffusion rate. Therefore, higher curing temperature produces coarser polymer network and generates PNLC with larger average domain size [10]. The anchoring force provided by polymer network becomes weaker with a larger domain size and coarser polymer network, and thus the driving voltage decreases [11]. Based on the multi-layer model, free relaxation time (τ) is insensitive to the cell gap and it is governed by the average domain size (d_1) as:

$$\tau = \gamma_1 d_1^2 / (K_{11}\pi^2), \quad (1)$$

where γ_1 is the rotational viscosity, K_{11} is the splay elastic constant and d_1 is the average domain size. Therefore, the average domain size at each curing temperature can be obtained by measuring the free relaxation time of the PNLC. The time dependent phase relaxation curve can be expressed as $\delta(t) = \delta_0 \exp(-2t/\tau)$. Therefore, the free relaxation time for each PNLC sample can be extracted. Next, we calculated the average domain size based on Eq. (1).

Fig. 1(b) depicts the domain size obtained at each curing temperature. As the curing temperature increases from 0°C to 70°C, the average domain size increases from 130nm to 280nm because of the increased monomer diffusion rate. The increased domain size has pros and cons. On the positive side, it weakens the anchoring force, leading to a lower operation voltage. But on the negative side, the response time increases. From Fig. 1(b), even the curing temperature reaches 70°C the domain size is only 280nm, which is still much smaller than the infrared wavelength (λ=1.55μm). Thus, light scattering remains negligible. Based on Stokes-Einstein theory, the domain size is inversely proportional to the viscosity. Thus, the domain size (d_1) can be expressed as $d_1^2 \sim T/\eta$, here, T is the Kelvin temperature and η is the flow viscosity. The flow viscosity is also temperature dependent as $\eta \sim (1-T/T_c)^{\beta} \cdot \exp(E_b/k_B T)$, E_b is the fitting parameter related to activation energy, T_c is the clearing point, and β is a material constant. Therefore, the curing temperature dependent domain size is expressed as [12]:

$$d_1 = A \cdot \sqrt{\frac{T \exp(-E_b/k_B T)}{(1-T/T_c)^{\beta}}}, \quad (2)$$

where A is a fitting parameter. We fitted average domain size d_1 at various curing temperatures with Eq. (2). Good agreement is obtained as shown in Fig. 1(b). The fitting parameters are A=106.9 $nm/\sqrt{K}$ and E_b=131.3 meV. The material constant β=0.16 is obtained independently by fitting the temperature dependent birefringence data. The adjustable parameter A is governed by the viscosity of LC host, monomer concentration, and UV dosage. [13] Besides, the threshold voltage (V_{th}) is inversely proportional to d_1. Thus, we fitted the threshold voltage at each curing temperature with following equation:

$$V_{th} = \frac{B}{d_1} = B\sqrt{\frac{(1-T/T_c)^{\beta} \exp(E_b/k_B T)}{T}}, \quad (3)$$

here B is a fitting parameter, while T_c and β maintain unchanged. As shown in Fig. 1(a), good agreement is obtained with B=26.5 $V\sqrt{K}$ and E_b = 137.5 meV. The obtained activation energy is within 5% of that fitted with Eq. (2), which confirms the validity of our physical model between domain size and curing temperature. Since both operation voltage and response time are determined by the domain size, this physical model provides useful guidelines to optimize the domain size by controlling curing temperature.

When the curing temperature is further increased to 73°C, $V_{2\pi}$ drops to 22.8V, as Fig. 2(a) shows, which is within the reach of LCoS. Fig. 2(b) shows the measured decay time of a reflective PNLC cell whose initial biased voltage is 22.8V. The measured phase decay time (from 100% to 10%) is 1.13ms, which is ~100X faster than that of the corresponding nematic device.

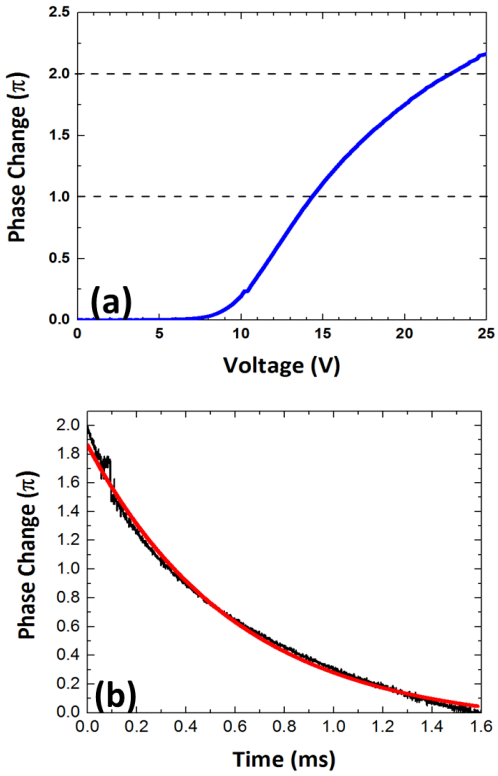

Figure 2 (a) Voltage-dependent phase curve of a PNLC cured at 73°C with $V_{2\pi}$ =22.8V. (b) Measured phase decay time of the PNLC sample.

Figure of Merit (FoM) of LC Host

Table 1. Physical properties and figure of merits of five LC hosts used in PNLCs.

LC mixtures	Δn (λ=633nm)	$\Delta\varepsilon$	γ_1 (Pa·s)	FoM_1 ($\Delta\varepsilon\Delta n^2/\gamma_1$) $(Pa\cdot s)^{-1}$	FoM_2 ($\Delta\varepsilon/\gamma_1$) $(Pa\cdot s)^{-1}$
HTG135200 (HCCH)	0.21	86	1.20	3.16	71.67
JC-BP07N (JNC)	0.17	302	3.88	1.82	77.84
E44 (Merck)	0.24	16	0.33	2.79	48.48
BL038 (Merck)	0.25	16	0.56	1.79	28.57
BP1(HCCH)	0.15	50	1.52	0.74	32.89

The overall performance of a PNLC device is governed by three key parameters: 1) 2π phase change, 2) low operation voltage, and 3) fast response time. Besides the cell gap and domain size, the physical properties of LC host also play a key role in determining the overall performance of PNLC. As discussed above, the domain size can be controlled by the monomer concentration and curing temperature. If a certain phase change (say δ=2π) is required, then the cell gap should satisfy d=λ/Δn. To balance the overall performance, voltage and response time need to be considered. To eliminate the domain size effect, here we define a Figure of Merit (FoM_1) as:

$$FoM_1 = 1/(V_{2\pi}^2 \tau) \sim \Delta\varepsilon\Delta n^2/\gamma_1. \quad (4)$$

From Eq. (4), LC host with a large $\Delta\varepsilon$, Δn and small γ_1 is preferred for PNLC devices. If the cell gap is fixed, then FoM_1 could be simplified to:

$$FoM_2 = 1/(V_{2\pi}^2\tau) \sim \Delta\varepsilon/\gamma_1. \quad (5)$$

Table I lists several LC hosts we employed for making PNLC devices. HTG 135200 (HCCH, China) shows the highest FoM_1 among those LC mixtures due to its relatively high birefringence and dielectric anisotropy. However, if the cell gap is fixed, then JC-BP07N shows the best performance due to its extremely large $\Delta\varepsilon$. Thus, for λ=1.55μm and d=11.8μm, JC-BP07N is a good host. When the curing temperature is increased to 73°C, the operation voltage is reduced to below 24V. Besides, FoM_1 and FoM_2 are sensitive to the temperature because Δn, γ_1 and $\Delta\varepsilon$ are temperature dependent as

$$\Delta n = \Delta n_0 S = \Delta n_0 (1 - T/T_c)^{\beta}, \quad (6)$$

$$\gamma_1 \sim S \cdot \exp(E_a/k_B T), \quad (7)$$

$$\Delta\varepsilon = C \cdot S \exp(U/k_B T), \quad (8)$$

where S is the order parameter, Δn_0 is the extrapolated birefringence at T=0K, C is a fitting parameter, and U is a parameter related to the dipole moment. By combining these equations, the temperature dependency of FoM_1 is derived as:

$$FoM_1 = D \cdot \frac{(1 - T/T_c)^{2\beta}}{\exp((E_a - U)/k_B T)}, \quad (9)$$

here D is a fitting parameter.

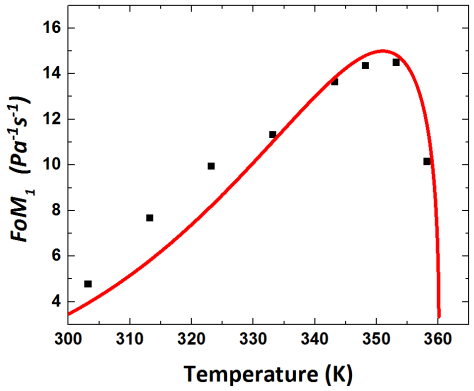

Figure 3 Temperature dependent FoM_1 for JC-BP07N at λ=633nm: dots stand for the measured data and red line for fitting curve with Eq. (8)

As shown in Fig. 3, dots stand for the measured data and red line for the fitting results with Eq. (9) for JC-BP07N. Good agreement is obtained with following fitting parameters: D=8.98×10^6, U=207.8 meV, E_a=575.3 meV, β=0.16 and T_c=87°C. Since the polymer network (i.e. domain size) and device structure are independent of operating temperature, the temperature dependent performance of PNLC is basically determined by the employed LC host only. As the temperature increases, viscosity decreases more quickly than birefringence and dielectric anisotropy initially, resulting in an increased FoM_1. As T approaches T_c, Δn decreases more quickly than γ_1, leading to a sharply declined FoM_1. Therefore, for a given PNLC an optimal operation temperature (T_{op}) exists which gives the maximum FoM_1. To derive the optimal temperature, we set $d(\mathrm{FoM})/\mathrm{dT} = 0$ and find that

$$T_{opt} = T_c - \frac{2\beta k_B T_c^2}{E_a - U}. \quad (10)$$

By substituting the fitting parameters of JC-BP07N, we found T_{op}=77.4°C. At T_{op}, FoM_1 has a peak value even though the operation voltage would increase due to the decreased $\Delta\varepsilon$. Therefore, the device can be operated at T_{op} if fast response time is the primary requirement.

3. Summary

We report a reflective mode PNLC phase modulator with $V_{2\pi}$ =22.6V and response time ~1ms, which will allow PNLC to be integrated in a high resolution LCoS for next generation SLM applications. Besides, the paper also provides a guideline to choose LC host and optimize curing conditions for fabricating PNLC spatial light modulators.

4. Acknowledgement

The authors are indebted to AFOSR for the financial supports under contract No. FA9550-14-1-0279.

5. References

[1] U. Efron, *Spatial light modulator technology: materials, devices, and applications* (Marcel Dekker, New York, 1994).

[2] S. Quirin, D. S. Peterka, and R. Yuste, "Instantaneous three-dimensional sensing using spatial light modulator illumination with extended depth of field imaging," Optics Express **21**(13), 16007-16021 (2013).

[3] F. Feng, I. H. White, and T. D. Wilkinson, "Free space communications with beam steering a two-electrode tapered laser diode using liquid-crystal SLM," Journal of Lightwave Technology **31**(12), 2001-2007 (2013).

[4] B. M. Moslehi, K. K. Chau, and J. W. Goodman, "Optical amplifiers and liquid-crystal shutters applied to electrically reconfigurable fiber optic signal processors," Optical Engineering **32**(5), 974-981 (1993).

[5] F. Peng, Y. Chen, S.-T. Wu, S. Tripathi, and R. J. Twieg, "Low loss liquid crystals for infrared applications," Liquid Crystals **41**(11), 1545-1552 (2014).

[6] J. Sun and S. T. Wu, "Recent advances in polymer network liquid crystal spatial light modulators," Journal of Polymer Science Part B: Polymer Physics **52**(3), 183-192 (2014).

[7] F. Peng, H. Chen, S. Tripathi, R. J. Twieg, and S.-T. Wu, "Fast-response infrared phase modulator based on polymer network liquid crystal," Optical Materials Express **5**(2), 265-273 (2015).

[8] Y.-H. Fan, Y.-H. Lin, H. Ren, S. Gauza, and S.-T. Wu, "Fast-response and scattering-free polymer network liquid crystals for infrared light modulators," Applied Physics Letters **84**(8), 1233-1235 (2004).

[9] S. A. Serati, X. Xia, O. Mughal, and A. Linnenberger, "High-resolution phase-only spatial light modulators with submillisecond response," Proc. SPIE **5106**(138-145 (2003).

[10] F. Du and S.-T. Wu, "Curing temperature effects on liquid crystal gels," Applied Physics Letters **83**(7), 1310-1312 (2003).

[11] D.-K. Yang, Y. Cui, H. Nemati, X. Zhou, and A. Moheghi, "Modeling aligning effect of polymer network in polymer stabilized nematic liquid crystals," Journal of Applied Physics **114**(24), 243515 (2013).

[12] F. Peng, D. Xu, H. Chen, and S.-T. Wu, "Low voltage polymer network liquid crystal for infrared spatial light modulators," Optics Express **23**(3), 2361-2368 (2015).

[13] I. Dierking, "Polymer network–stabilized liquid crystals," Advanced Materials **12**(3), 167-181 (2000).